Structural and Conformational Dependence of Optical Rotation Angles

Rama K. Kondru, Peter Wipf,* and David N. Beratan*

Department of Chemistry, University of Pittsburgh, Pittsburgh, Pennsylvania 15260

Received: February 26, 1999; In Final Form: April 28, 1999

The ability to compute and to interpret optical rotation angles of chiral molecules is of great value in assigning relative and absolute stereochemistry. The molar rotations for an indoline and an azetidine, as well as for menthol and menthone, were calculated using ab inito methods and compared to the experimental values. In one case the calculated rotation angle allowed the assignment of the absolute configuration of a heterocycle of unknown stereochemistry. The critical importance of Boltzmann averaging of conformers for reliable prediction of the optical rotation angle was established. Comparisons between static-field and time-dependent methods were made pointing to the limits and validity of the methods as electronic resonance is approached. A protocol analogous to population analysis was used to analyze atomic contributions to the rotation angle in specific conformers. The combination of atomic contribution maps and conformational analysis may provide an indirect tool to assist in three-dimensional structure determination.

I. Introduction

Many empirical,[1−6] semiempirical,[7−12] classical,[13,14] and quantum mechanical[15−22] models have been developed to predict and interpret chiroptical data. Quantitatively reliable quantum chemical computations of molar rotation angles have only very recently begun to impact the field.[23−26] Ab initio calculations of rotation angles appeared in 1997 in the long-wavelength (off-resonance) approximation for small molecules with one or two chiral centers.[23] We subsequently devised an ab initio approach to assign the configuration of a complex natural product by *calculating* molar rotation angles.[27] Recently, ab initio methods were used as well to map out the frequency dependent ORD spectrum of methylcyclohexanone.[28] The present paper examines the geometry dependence of computed rotation angles for a range of carbocyclic and heterocyclic organic molecules. We show that (1) computed optical rotation angles are very sensitive to geometry, (2) proper geometry sampling is essential for reliable prediction of observed rotations, (3) static-field methods are limited near resonant absoption, and (4) twisted chains remote from the chiral centers have a profound influence on the rotation angle.

The basic framework governing chiroptical phenomena in molecules was established in the early days of quantum mechanics by Rosenfeld and Condon.[29,30] In the following decade, numerous qualitative and semiquantitative models were elaborated that addressed, with differing degrees of success, the relation between structure and rotation angle. In the 1940s, the possibility of directly computing rotation angles seemed bleak because of the paucity of reliable molecular wave functions.[31] Direct applications of the Rosenfeld equation must have seemed particularly challenging at the time because it includes a sum over *all* molecular excited states.

In principle, ORD (optical rotatory dispersion) and CD (circular dichroism)[4] data, in combination with other structural information, can be used to establish absolute stereochemistry.[3,4] CD, in particular, has been used successfully to assist in assigning the configuration of many complex natural products.[4,32] Conformational analysis of biomolecules based upon CD spectroscopy is well-known.[33−35] In practice, however, assigning stereochemistry remains a formidable challenge and methods complementary to NMR, X-ray, and other spectroscopic techniques are clearly desirable.

To determine absolute configuration, one must first know the chemical constitution (bonding pattern), the molecular conformation, and the "rules" controlling chiroptical effects for a given class of molecules under study. Emerging spectroscopic methods such as VCD (vibrational CD) do not yet offer substantial advantages for large organic molecules with multiple stereocenters and require considerably more elaborate instrumentation.[36,37] The ORD spectrum is an appealing source of stereochemical information because it reflects the global features of a molecule's chiral environment. In contrast, stereochemical information obtained from the CD spectra of small molecules reflects the stereochemical environment around specific chromophores. Moreover, solvent absorption <200 nm obscures CD spectra in many organic molecules of interest in natural products chemistry. The simplicity of examining $[\alpha]_D$, and its comprehensive probing of stereochemistry, makes it a particularly appealing spectroscopy on which to focus theoretical attention. Empirical correlations have been constructed that link the molar rotation at a given wavelength (a single point in the ORD spectrum) with chemical structure. One of the oldest and simplest empirical rules is van't Hoff's principle of optical superposition.[1] This rule suggests simple arithmetic summation of molar rotations for each noninteracting chiral center as an approximation of the molar rotation of a species with multiple stereocenters. Obvious shortcomings such as the vicinal action limitation have greatly restricted general applications of van't Hoff's rule.

The best known quantitative rules linking chemical structure to the rotation angle through additive contributions are Brewster's rules.[38] The Brewster model is based upon individual atomic polarizabilities. Obvious limitations to schemes of this kind arise when the assumed polarizabilities are not transferable (as in systems with somewhat novel chemical bonding) or when the geometric assumptions built into the model do not adequately describe the actual conformations of the molecule. Other qualitative trends are known as well. Eyring and Kauzmann

10.1021/jp990697e CCC: $18.00
Published on Web 08/03/1999

drew a link between rigidity and rotation angle.[39] Stevens has described the conformational dependence of ORD spectra.[40]

Our strategy involves the quantum mechanical computation of optical rotation angles at the sodium D-line (rather than the full ORD spectrum, although recent progress has been made in that direction as well[41]) for the specific molecules of interest. The optical rotation angle measures the difference in the index of refraction for left and right circularly polarized light in a solution of chiral molecules. The optical rotation angle is a probe of how the electron cloud responds dynamically to the oscillating electromagnetic fields. Atomic contributions to the optical rotational angle can now be computed using ab initio Hartree−Fock methods.[42] Most computational strategies follow along two basic lines. One involves computing a sum-over-excited-states expression, and the second involves a linear response approach (in a time-dependent or time-independent framework).[24,27] The specific calculations that we describe here rely critically upon sampling among energetically accessible conformers. The computed "observable" rotations are weighted averages of values computed for specific structures. For a specific conformer, the optical rotation angle can be dissected into atomic contributions.[42] These atomic contributions allow dissection of angle contributions into chiral center components and components arising from asymmetric fragments that contribute to optical activity by virtue of their asymmetric twists.

II. Theoretical Methodology

Both the sign and the order of magnitude of the rotation angle can now be computed for modestly sized chiral molecules.[24−27] The optical rotation angle may be computed from the electric- and magnetic-field derivatives of the ground-state electronic wave function, $\partial\Psi/\partial E_\alpha$ and $\partial\Psi/\partial B_\alpha$, within the static-field approximation. Recent numerical computations capitalize on techniques that were developed to compute vibrational Raman optical activity within the CADPAC program.[43] The long-wavelength approximation can be relaxed using alternative linear-response methods, and our preliminary computations show that the calculations (utilizing the ab initio software package, DALTON)[44] are generally in accord with the long-wavelength results.

The expression for the optical rotational angle, ϕ in radians, is[29]

$$\phi = 4\pi N\beta\omega^2(n^2+2)/3c^2 \tag{1}$$

where

$$\beta = -\omega^{-1}(G'_{xx}+G'_{yy}+G'_{zz})/3 \tag{2}$$

G'_{ii} are the diagonal elements of the electric-magnetic polarizability tensor.[24] N is the number of molecules per unit volume, n is the refractive index of the medium, and c is the speed of light. The specific rotation angle (measured at the sodium D-line), in units of degrees [dm (g/mL)]$^{-1}$, is

$$[\alpha]_D = 1.343\times10^{-4}\beta\bar{\nu}^2(n^2+2)/3\mathrm{MW} \tag{3}$$

with β in units of (bohr),[4] MW the molar mass in g/mol, and $\bar{\nu}$ the frequency of the sodium D-line in cm^{-1}.[24] From $[\alpha]_D$, the molar rotation is defined as $[M]_D = [\alpha]_D\mathrm{MW}/100$. We calculate $G'_{\alpha\alpha}$ for the full molecule using

$$G'_{\alpha\alpha} = -2\sum_{e\neq g}\frac{\omega\ \mathrm{Im}[\langle\Psi_g^{(0)}|\mu_\alpha|\Psi_e^{(0)}\rangle\langle\Psi_e^{(0)}|m_\alpha|\Psi_g^{(0)}\rangle]}{\omega_{eg}^2-\omega^2} \tag{4}$$

Here, g and e denote the ground state and eth excited states, respectively, $\omega_{eg} = \omega_e - \omega_g$ is the associated excitation frequency, and μ and m are the electric−dipole and magnetic−dipole operators oriented along the α-axis.

A. Static-field approximation. To avoid the explicit sum-over-states expression for the electric dipole−magnetic dipole polarizability tensor, Amos applied the static field approximation. In this regime, eq 4 is simplified ($\omega^2 \ll \omega_{jn}^2$)[45]

$$\omega^{-1}G'_{\alpha\alpha} = -2\sum_{e\neq g}\frac{\mathrm{Im}[\langle\Psi_g^{(0)}|\mu_\alpha|\Psi_e^{(0)}\rangle\langle\Psi_e^{(0)}|m_\alpha|\Psi_g^{(0)}\rangle]}{\omega_{eg}^2} \tag{5}$$

and by writing $\omega_{eg} = (E_e(0) - E_g(0))$ in eq 5, we obtain

$$\omega^{-1}G'_{\alpha\alpha} = -2\mathrm{Im}\sum_{e\neq g}\left\{\frac{\langle\Psi_g^{(0)}|\mu_\alpha|\Psi_e^{(0)}\rangle}{(E_e^{(0)}-E_g^{(0)})}\right\}\left\{\frac{\langle\Psi_e^{(0)}|m_\alpha|\Psi_g^{(0)}\rangle}{(E_e^{(0)}-E_g^{(0)})}\right\} \tag{6}$$

The electric dipole−magnetic dipole polarizability tensor elements $G'_{\alpha\beta}$ are most easily interpreted in the static-field approximation in terms of first-order changes induced to an electronic state by applied electric and magnetic fields (those terms in the brackets of eq 6 are equivalent to first-order perturbation theory wave function mixing terms). These tensor elements are computed in the CADPAC program of Amos.[43]

B. Frequency-Dependent Formulation. The frequency-dependent electric dipole-magnetic dipole polarizability tensor elements $G'_{\alpha\alpha}$ of eq 4 are calculated at the frequency of the incident light using the linear-response method realized in the DALTON program.[44] The electric dipole-magnetic dipole polarizability tensor can be expressed in terms of the linear-response function as[46,47]

$$G'_{\alpha\alpha} = -\langle\langle\mu_\alpha;m_\alpha\rangle\rangle = -\sum_j\left[\frac{\langle n|\mu_\alpha|j\rangle\langle j|m_\alpha|n\rangle}{\omega-\omega_{jn}} - \frac{\langle n|m_\alpha|j\rangle\langle j|\mu_\alpha|n\rangle}{\omega+\omega_{jn}}\right] \tag{7}$$

In this expression, n and j denote the ground and excited states and $\omega_{jn} = \omega_j - \omega_n$ is the associated excitation frequency. Here μ_α and m_α are electric dipole and magnetic dipole interaction operators, respectively.[48,49] Using the SCF linear-response method avoids the need to compute the excited-state wave functions of eq 6. This makes the computation tractable for organic molecules (or molecular fragments). G′ elements were computed both with (eq 6) and without (eq 7) the long-wavelength approximation.[23,50] London atomic orbitals (gauge-invariant atomic orbitals) were used to calculate the gauge origin independent G′tensor elements.[51,52]

C. Atomic Contributions to the Optical Rotation Angle. $\mathbf{G'_{\alpha\alpha}}$ is most easily interpreted in terms of first-order changes induced in the electronic ground state by applied electric (E) and magnetic fields (B). For a single-determinant wave function, first-order changes to the ground state are described in terms of perturbations to the molecule's occupied molecular orbitals. These are

$$\frac{\partial\psi_n}{\partial E_\alpha} = \sum_{j\neq n}\left\{\frac{\langle\psi_n^{(0)}|\mu_\alpha|\psi_j^{(0)}\rangle}{(E_j^{(0)}-E_n^{(0)})}\right\}\psi_j^{(0)} = \sum_{j\neq n}P_{nj}\psi_j^{(0)} \tag{8a}$$

$$\frac{\partial\psi_n}{\partial B_\alpha} = \sum_{j\neq n}\left\{\frac{\langle\psi_n^{(0)}|m_\alpha|\psi_j^{(0)}\rangle}{(E_j^{(0)}-E_n^{(0)})}\right\}\psi_j^{(0)} = \sum_{j\neq n}Q_{nj}\psi_j^{(0)} \tag{8b}$$

Here, n and j represent the nth occupied and jth unoccupied molecular orbitals, respectively. The P and Q elements are computed routinely using coupled-perturbed Hartree−Fock methods, within the CADPAC program library.[43] The G′ tensor elements is related to the overlap of the wave function derivatives (eq 6).[53] Moreover, the change can be cast in terms of specific atomic orbital contributions[42] as shown in eq 9.

$$\omega^{-1}G'_{\alpha\alpha} = -2\mathrm{Im}\left\{\sum_n \left\langle \frac{\partial\psi_n}{\partial E_\alpha}\middle|\frac{\partial\psi_n}{\partial B_\alpha}\right\rangle\right\} = -2\sum_n\sum_{l,k} P'_{nl}Q'_{nk}\langle\phi_l|\phi_k\rangle \tag{9}$$

As in the case of population analysis, eq 9 can be dissected into atomic orbital, atom, bonding and through-space contributions.[54]

D. Conformational Search Using MacroModel. Our analysis seeks to combine the results of quantum chemical calculations on a limited number of molecular conformations to estimate an ensemble averaged molecular quantity. Since we are unable to perform a full ensemble average, we attempt to replace it with an average over minimum energy conformers that are thermally accessible from the minimimum energy conformer. This strategy neglects entropic contributions to the free energy associated with different conformers, and this effect can be of particular importance in sampling structures of considerable flexibility. This approach toward geometry sampling should be viewed as part of the "hypothesis" implicit in our approach. It is only a first step toward a more complete hybrid quantum/statistical mechanical approach to the problem.

Unique low energy geometries were obtained from Monte Carlo conformational searches using the Macromodel[55] program with the MM2* force field parametrization. This force field is believed to produce relative energies of high reliabitity.[56] The result of utilizing alternative force fields is under investigation. After building the required structure with appropriate configuration, it was minimized using the MM2* force field and an energy minimization algorithm (PRCG).[55] This minimized structure was then submitting to a stochastic search. The conformers obtained by Monte Carlo sampling were minimized at every step and compared to see if the newly obtained structure was duplicated.[55] If so, the duplicated structure was ignored. Only unique structures were retained. Low energy structures were usually chosen from a Monte Carlo sampling of 2000 conformations, each new conformation was minimized using a 2000 step energy minimization iteration method forcing all the newly found structures to be fully relaxed. All the conformations generated within a few kT (those thermally accessible in solution) are used in the optical rotational angle computations. MacroModel treats solvent using a fully equilibrated analytical continuum model starting near the van der Waals surface of the solute.[57] This model is also known as the GB/SA model and includes the parameters for one high dielectric solvent and one lower dielectric solvent (water and chloroform). One of the major sources of errors in conformational search methods is carrying out a calculation which is unconverged. Such calculations give significantly different answers for different initial input conditions. This conformational searching strategy represents geometries accurately for structures with up to a dozen flexible bonds, but it becomes problematic as more conformational freedom is added. To overcome this limitation, the number of minimization iterations for each conformer that is generated with Monte Carlo sampling was set to 2000 steps. In most cases, for the molecules reported in this paper multiple searches were carried out with different starting configurations (R or S) as a means of probing the adequecy of geometric sampling. If sampling were perfect, the results would be exactly equal in magnitude but opposite in sign. Using multiple starting geometries of the same configuration repeatedly would produce the same statistical analysis. Experimental measurements of specific rotation angles arise from the thermally accessible conformers in solution. Hence, in our calculations the specific rotational angles are computed using the geometries of the conformations generated using the Monte Carlo search and are Boltzmann summed to obtain the final computed specific rotation for the configuration of the compound. The Boltzmann sum is obtained using

$$[\alpha]_D^{\mathrm{Boltz\_summ}} = \frac{\sum_i e^{-E^{(i)}/kT} \times [\alpha]_D{}^{(i)}}{\sum_i e^{-E^{(i)}/kT}} \tag{10}$$

Here, k is Boltzmann's constant, T is the temperature, $E^{(i)}$ is the relative energy of the conformer, and $[\alpha]_D{}^{(i)}$ is the specific rotation computed for the individual conformer. It is important to note that the specific rotation angles of individual conformations $[\alpha]_D{}^{(i)}$ are distinct for each conformer, differing in both sign and magnitude. Lower energy conformations that are much more highly populated have the largest impact on this sum.

III. Results and Discussion

A. Absolute Configuration of an Indoline. The absolute stereochemistry of indoline (**1**) was not known prior to our

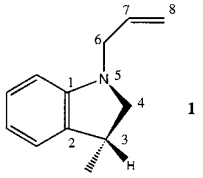

1

(*R*)-indoline

calculation.[58] It was a particular challenge to predict the specific rotation of this molecule because of the flexibility of the five-membered ring and the double bond separated by a flexible methylene unit. It is important to note that the chiral center at C3 is perturbed by ring flips as well as by the freely rotating substituent that contains the double bond.

(i). Importance of Conformational Search. The specific rotation of indoline, **1**, was measured experimentally in methylene chloride.[58] The five-membered ring and the C_3H_5 group attached to the nitrogen lead to considerable structural flexibility. Low energy geometries for the (*S*)- and (*R*)-configurations were obtained from Monte Carlo conformational searches using the MacroModel[55] algorithm with the MM2* force field. Low energy structures were chosen from a sampling of 2000 conformations with chloroform as the solvent (as described in section IID). Conformational search with methylene chloride as the continuum solvent was not available in MacroModel, so the chloroform model was chosen. For many organic molecules $[\alpha]_D$ is very similar in chloroform and methylene chloride.[59] In the case of indoline, $[\alpha]_D$ measurements in chloroform might not provide ideal comparison because of the possibility of amine protonation by traces of HCl in the solvent. Figure 1 shows the low energy structures obtained from the conformational search. We find two distinct classes of conformers that differ in the puckering of the five-membered ring. Approximately half of the conformations have the five-membered ring puckered up and half down. Table 1 shows the importance of conformational

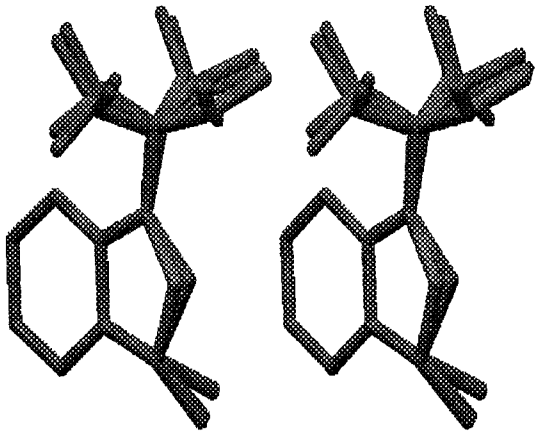

Figure 1. Overlayed stereoview of the thermally accessible (R)-indoline (**1**) conformations.

averaging to obtain meaningful optical rotation angles. For the (*R*)-isomer of indoline (**1**), the MM2* energy of the next to lowest conformer is 0.22 kJ/mol above the minimum. The conformer ranked with the 16th lowest energy is 3.74 kJ/mol above the minimum. It is evident that all of these conformations are very much accessible in solution. To improve the accuracy of the computation, all calculations were independently repeated for the (*S*)-isomer, which showed a closely related energy distribution. Molar rotation angles for all conformations were computed using the static-field limit described in section IIA.

(ii). Specific Rotation Angles in the Static-Field Formulation. The electric dipole-magnetic dipole polarizability tensor described in eq 4 was computed using the CADPAC program. These tensor elements were used to calculate the optical rotatory parameter β (eq 2) for all low-energy conformations of **1**. Finally, the specific rotations of the 16 low energy conformations were Boltzmann weighted and summed to compute the specific rotation of (*R*)- and (*S*)-indoline. Table 1 shows the specific rotation at the sodium D-line (589.3 nm), the energy of each conformation, and the Boltzmann averaged angle for the (*R*)-configuration. The low energy conformations that were generated in the range of 50 kJ/mol for (*R*)- and (*S*)-configurations of **1** were included in the Boltzmann sum. In all, the Monte Carlo search found 19 low energy conformers for the (*S*)- and 16 for the (*R*)-configuration. For the S-configuration, the three highest energy structures were found only once and make essentially no contribution to the specific rotation angle. All lower energy conformers that are found for one enantiomer have a near mirror image structure that is found for the enantiomer. The Boltzmann averaged specific rotation for the (*S*)-configuration is 67.9 and for (*R*)-**1** it is −64.0. Experimentally, the Bailey group determined a specific rotation of −59.0 for **1**. The theoretical computations allow the assignment of this stereoisomer as (*R*). Small differences in the computed optical rotations of the (*R*)- and (*S*)-isomers are attributed to the fact that the conformational sampling is randomized and of course imperfect. However, attempting to predict absolute stereochemistry based upon any one conformer would clearly be inappropriate and misleading for compounds of this class. The specific rotation values for different conformers differ in both their sign and substantially in their order of magnitude.

Table 2 shows the theoretically computed and the experimentally determined specific rotation angles for (*R*)-indoline (**1**) at four different incident wavelengths. All of these optical rotation angles are computed using the coupled Hartree−Fock method with a 6-31G* basis set. The electric dipole−magnetic dipole polarizability tensor and the optical rotatory parameter

TABLE 1: Specific Rotation Angles Computed for the 16 Low Energy Conformations of (*R*)-Indoline (1) Using the Long Wavelength Approximation (CADPAC) and the Linear-Response Method (DALTON)

CONF	$E^{(i)}$ (kJ/mol)	$[\alpha]_D^{(i)}$ (CADPAC)	$[\alpha]_D^{\text{Boltz\_sum}}$ (CADPAC)	$[\alpha]_D^{(i)}$ (DALTON)	$[\alpha]_D^{\text{Boltz\_sum}}$ (DALTON)
1(a)	0.0	120.90	120.90	160.83	160.83
2(b)	0.22	−347.28	−102.67	−402.26	−108.06
3(c)	0.58	258.05	2.43	314.62	15.10
4(d)	0.67	−243.11	−51.33	−290.10	−51.73
5(e)	1.50	−529.02	−115.55	−613.00	−127.18
6(f)	1.71	321.57	−67.56	329.79	−70.10
7(g)	2.09	−491.38	−103.97	−580.13	−113.91
8(h)	2.13	361.49	−67.81	424.56	−72.09
9	2.58	−37.93	−66.00	−48.39	−77.35
10	2.59	−158.35	−71.26	−158.94	−75.70
11	2.89	72.53	−64.38	98.38	−67.37
12	3.07	−114.35	−66.51	−106.90	−69.05
13	3.09	−4.09	−63.98	−16.29	−69.91
14	3.61	−163.78	−67.13	−156.09	−69.73
15	3.70	−151.10	−69.61	−174.52	−72.82
16	3.74	127.39	−64.04	130.48	−67.07

[a] Also shown are the relative conformational energy (*E*) and the Boltzmann weighted sum (Boltz_sum) as the specific rotation of each conformer is added to the sum. Letters in the first entry refer to Figure 4. Note that among the 8 lowest energy conformers, half contribute negative rotation angles while half contribute positive values, despite the fact that the overall (*R*)- or (*S*)-configuration is retained. The analysis of the geometry for each of these conformations with regard to the optical rotation provides an interesting clue essential for understanding the origin of the sign of the observed optical rotation angle.

TABLE 2: Experimental and Computed Specific Rotation Angles (Boltzmann Averaged) for (*R*)-Indoline (1) Computed Using the Long Wavelength Approximation (CADPAC) and the Linear-Response Method Using London Atomic Orbitals (DALTON) for Four Different Incident Light Frequencies[58]

wavelength (nm)	$[\alpha]_D$ (CADPAC)	$[\alpha]_D$ (DALTON)	$[\alpha]_D$ exptl (*R*)[58]
589	−64.04	−67.07	−59.0
577	−66.80	−71.05	−68.2
546	−74.60	−82.92	−82.2
435	−117.52	−167.97	−208.2

(β) are calculated using the static-field approximation. As shown in eq 2, the specific rotation is proportional to the square of ω. All the values of specific rotations computed using the CADPAC program (shown in Table 2) are computed by simply scaling β obtained in the long-wavelength approximation as prescribed by eq 5. The theoretical value of the specific rotation computed using the CADPAC program for the (*R*)-configuration at 589 nm is −64.04 compared to the experimental value of −59.0. Theoretical values at 577 and 546 nm are −66.80 and −74.60, respectively, compared to experimental values of −68.2 and −82.2. The percent error between the theory and the experimental values increases as the frequency of the incident light approaches the lowest energy electronic resonance for the molecule. This divergence is expected because the theoretical values of β are computed using the long-wavelength approximation that is valid far from resonance. The CADPAC computed specific rotation at 435 nm is −117.52 as compared to the experimental value of −208.2. All specific rotation values shown in Table 2 for the (*R*)-configuration are Boltzmann weighted averages summed over all the conformations shown in Table 1.

(iii). Specific Rotation Angles Using the Frequency Dependent Method with Gauge Invariant Atomic Orbitals. The optical rotation angles for (*R*)- and (*S*)-configurations of indoline (1) were also computed using the linear response self-consistent field method implemented in the DALTON program. Gauge-

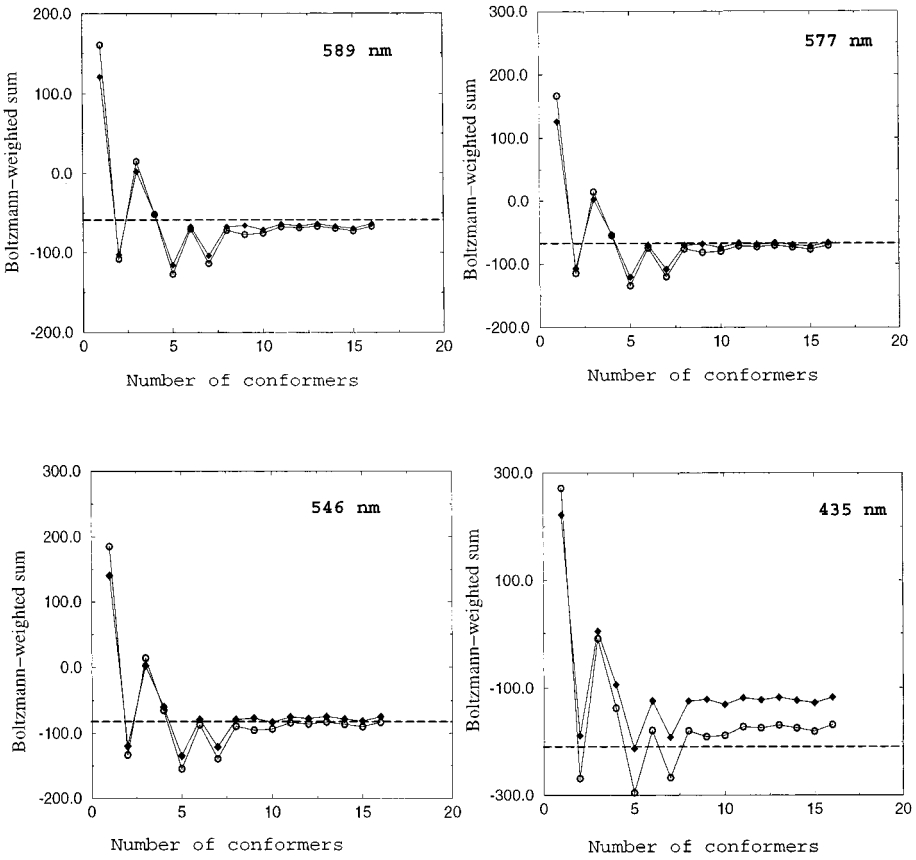

Figure 2. The computed Boltzmann-weighted sum for (*R*)-**1** at the incident light wavelength of 589, 577, 546, and 435 nm. The lines with circles show the Boltzmann-weighted average computed using the DALTON program, and the lines with filled diamonds show the results computed using the CADPAC program. The dashed line shows the experimentally measured specific rotation angle at the indicated wavelength.

invariant atomic orbitals (or London atomic orbitals) were used to compute the optical rotation angles. The optical rotation angles computed using London atomic orbitals are gauge independent. The optical rotatory parameter β is computed at the incident-light frequency. Hence, this method should more accurately predict the ORD spectrum as the incident frequency approaches electronic resonances.

Table 1 shows the computed specific rotation angles for the (*R*)-configuration of indoline (**1**) using London atomic orbitals. All results in Table 1 were computed at 589 nm. At this wavelength, both frequency dependent and frequency independent methods are in good agreement with the experimental results. As the incident frequency approaches the lowest energy electronic resonances, the long-wavelength approximation, of course, does not produce quantitatively reliable optical rotation angles. In such cases, it is more appropriate to employ the linear-response method implemented in the DALTON program. The Boltzmann weighted average of the specific rotation angle using DALTON at 589 nm for (*R*)-**1** is −67.1 compared to the experimental value of −59.0. Figure 2 shows the accumulating Boltzmann averaged sum of the specific rotation angle as each conformation is added to the Boltzmann summation for (*R*)-**1**. Specific rotation angles were computed at 589 nm, 577, 546, and 435 nm for (*R*)- and (*S*)-configurations of indoline using the CADPAC and DALTON methods. At 589 nm, both methods give rather similar results (the long-wavelength computation is less costly). At 435 nm, the deviation from the experimental values for the CADPAC result is large compared to that of DALTON.

The optical rotation angles for different conformers of indoline (**1**) varied considerably. It is of great interest to understand the structural origin of the sign and magnitude of

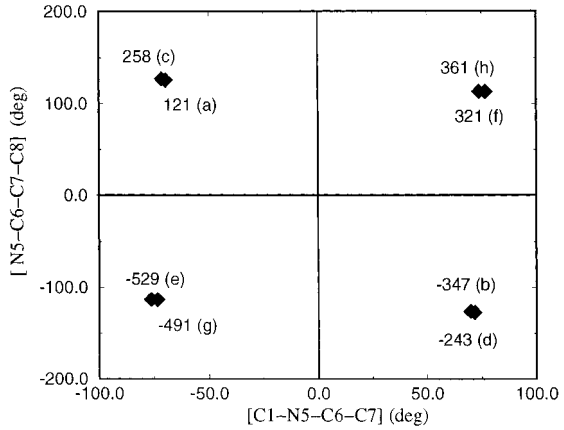

Figure 3. Dihedral angle plot showing the specific rotation angle dependence on the torsional angles for the eight low energy conformers of (*R*)-indoline. The labels indicate the computed specific rotation angles for the respective dihedral angle pair for conformers (**a**−**h**).

the optical rotation angle for a given conformer of **1**. The specific rotation angle for **1** converged to within 5% of the final value after including just eight low-energy conformers in the Boltzmann sum. Hence, we analyzed these eight low-energy conformers to identify fragments of this molecule that account for the sign change. Figure 3 shows a Ramachandran-like plot for the low energy conformers of (*R*)-indoline (**1**). The torsion angle C1−C2−C3−C4 reports the five-membered ring pucker. The torsion angles C1−N5−C6−C7 and N5−C6−C7−C8 reflect the conformation of the allyl group attached to the nitrogen. It is clear from Figure 3 that there are four clusters of rotation angles for these structures. The specific rotation angle sign change (*vide infra*) between the conformers is in phase

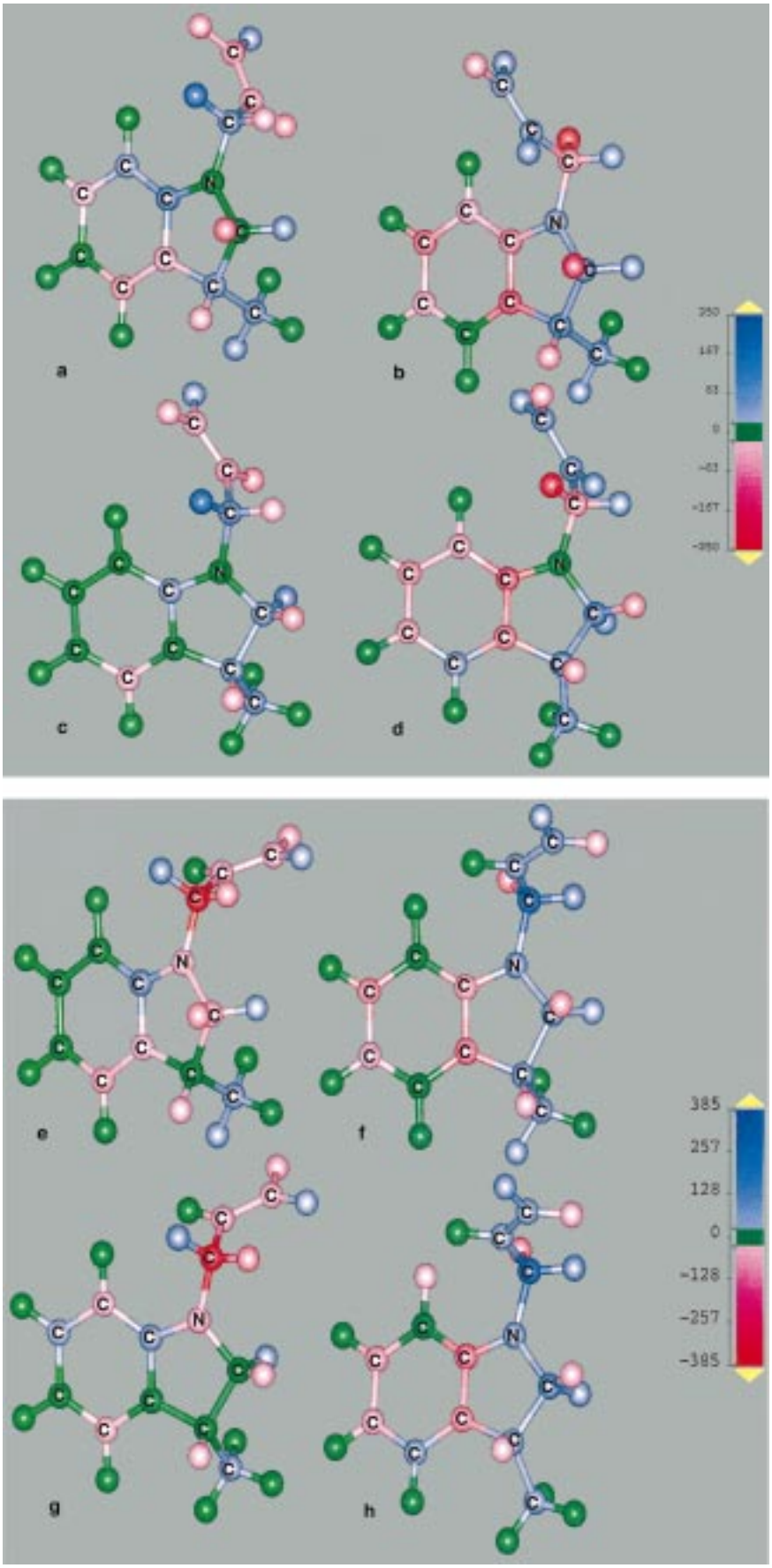

Figure 4. Atomic contributions to the specific rotation angle for the eight low energy conformers of (*R*)-indoline (**1**). Atoms that are green have small contributions, blue atoms have positive contributions, and red atoms have negative contributions to the specific rotation angle.

TABLE 3: Computed Molar Rotation Angles for Two Conformations (a, b) of 2-Methyl Azetidine in *cis*-(*R*)- and *trans*-(*S*)-Configurations Using the Long Wavelength Approximation with the Basis Sets 6-31G*, 6-31G, and DZP from the CADPAC Library[a]**

	6-31G*	6-31G**	DZP
cis-(*R*)-**2**(a)	−59.0	−50.1	−42.2
cis-(*R*)-**2**(b)	−59.3	−50.4	−42.6
trans-(*S*)-**3**(a)	−13.8	−7.0	−65.5
trans-(*S*)-**3**(b)	−13.9	−7.1	−65.5

[a] The geometries for the *cis*- and *trans*-conformations were optimized using ab initio Hartree−Fock methods with a Gaussian 6-31G* basis set.

TABLE 4: Computed Molar Rotation Angles for Two Conformations (a, b) of 2-Methyl Azetidine in *cis*-(*R*)- and *trans*-(*S*)-Configurations Using the Long Wavelength Approximation with the Basis Sets 6-31G*, 6-31G and DZP from the CADPAC Library[a]**

	6-31G*	6-31G**	DZP
cis-(*R*)-**2**(a)	−28.6	−23.7	−20.8
cis-(*R*)-**2**(b)	−37.2	−28.1	−33.1
trans-(*S*)-**3**(a)	−20.7	13.3	−60.7
trans-(*S*)-**3**(b)	−20.7	13.2	−60.7

[a] The geometries for the *cis*- and *trans*-conformations were optimized using the MP2 method with a 6-31G* basis set.

with the (N5− C6−C7−C8) torsion angle. The torsion angle C1−N5−C6−C7 affects the way that the phenyl group interacts with the double bond but does not influence the sign. In Figure 3, pairs that cluster extremely closely differ in the ring pucker only, indicating a weak influence of the pucker angle on optical rotation. This analysis shows that the allyl group attached to nitrogen is mainly responsible for the magnitude and the sign of the optical rotation in each conformer of **1**, again highlighting the need for conformational averaging in computing reliable specific rotation angles. Moreover, this observation emphasizes one critical inherent difficulty in most simple (single geometry) empirical models of optical activity.

(iv). Atomic Contributions and Relation to Rotation Angle Sign Change. Recently, we developed a method to compute the atomic contributions to the specific rotation angle in a molecule via eq 9.[42] The G′ tensor trace, proportional to the specific rotation, is divided into parts that arise from the various atoms. This analysis provides trace insight into structure−chiroptical property relationships. Figure 4 shows all of the atomic contributions to the specific rotation angle in the eight lowest-energy conformers of (*R*)-**1**. The atomic contributions to the specific rotation angle for the four lowest energy conformation of (*R*)-**1** appear in Figure 4, conformers **a**−**d**. Figure 4, conformers **e**−**h**, shows the atomic contributions to the specific rotation angle for the next four higher energy conformations. The specific rotation angles for conformers **a**, **c**, **f**, and **h** are positive, while those for conformers **b**, **d**, **e**, and **g** are negative. All of the hydrogens on the phenyl ring show small contributions to the specific rotation in each of the conformers. The chiral carbon and its methyl group make uniformly positive contributions to the optical rotation angle in all conformers. The nitrogen atom makes a small contribution. The sign of the specific rotation angle in these conformers arises mainly from the contribution of the allylic group attached to the nitrogen and, to a lesser extent, from the carbon atoms on the phenyl ring. The torsion angle N5−C6−C7−C8 is positive in conformers **a**, **c**, **f**, and **h** leading to positive rotation angles. In contrast this torsion angle is negative in conformers **b**, **d**, **e**, and **g**, which have negative optical rotation angles. Figure 4 shows substantial contributions from the phenyl ring in conformers **b**, **d**, **f**, and **h** that have a negative C1−N5−C6−C7 torsion angle. This torsion angle tracks the interaction of the double bond with the phenyl ring, which induces a large contribution from the phenyl ring itself. It is interesting to note that in conformers **a**−**d** the allylic hydrogen (reporter hydrogen) makes a large contribution to the rotation angle that has the same sign as that of the overall rotation angle for the conformer. In conformers **e**−**h** the allylic carbon contribution is large and similarly indicative of the sign of rotation.

B. Azetidine. We were interested in examining contributions to the rotation angle in smaller heterocyclic rings. The azetidine molecule has already attracted some theoretical interest.[26] The force field calculations suggest that there are two dominant conformations associated with the ring flip in the four-membered ring. The interconversion between conformations may lead to difficulties in computing reliable molar rotation angles. We used these molecules as a test case to evaluate the influence of different geometry optimization methods and basis sets. Molar rotation angles are computed for *cis*-(*R*)-2-methyl azetidine and *trans*-(*S*)-2-methyl azetidine.

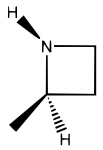

2

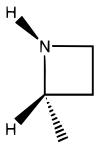

3

Table 3 shows the computed molar rotation angle for the two conformers of *cis*-(*R*)-2-methyl azetidine and *trans*-(*S*)-2-methyl azetidine. The geometries for these conformations were optimized using ab initio Hartree−Fock methods with a Gaussian 6-31G* basis set. The geometries for the two cis- and *trans*-conformers (a, b) differ by the ring torsion angle. These two different starting geometries converge to one low-energy geometry in the Hartree−Fock geometry optimization with a 6-31G* basis set implemented in Gaussian 94. The molar rotations were computed using the long-wavelength approximation. These calculations were performed using the 6-31G*, 6-31G**, and DZP basis sets from the CADPAC program library. An experimental molar rotation for *cis*-(*R*)-2-methyl azetidine is not available in the literature, but for *trans*-(*R*)-2-methyl azetidine, the experimental molar rotation is +3.0.[26,60] The molar rotation angle computed for *trans*-(*S*)-2-methyl azetidine using a 6-31G* basis set is −13.9 and with a 6-31G** basis set it is −7.1. These basis sets all give the observed experimental sign and approximate magnitude of the optical rotation. The computed molar rotation angle using the DZP basis set is −65.5. It is interesting to note that the value obtained from the DZP basis set is in agreement with the experimental molar rotation in sign but not in magnitude. This is distinct from the trend observed by Polavarapu in his calculations.[26] For *trans*-(*S*)-2-methyl azetidine, using a similarly optimized geometry and the long-wavelength approximation, and with 6-31G* and DZP basis sets, Polavarapu calculated molar rotation angles of +22.9 and −25.7, respectively.[26]

Table 4 shows a similar result as Table 3, except that the geometry optimization was carried out with MP2 level wave functions instead of Hartree−Fock wave functions. The computed molar rotation angles for *trans*-(*S*)-2-methyl azetidine using 6-31G*, 6-31G**, and DZP basis sets are −20.7, 13.2, and −60.7, respectively. There is not much difference from the corresponding numbers for 6-31G* and DZP basis sets (Table 3), but with the 6-31G** basis set, the sign of the angle changed from negative to positive, raising again the issue of basis set and geometry sensitivity in these molecules. These basis set

TABLE 5: Computed Molar Rotation Angles for Two Conformations (a, b) of 2-Methyl Azetidine in *cis*-(*R*)- and *trans*-(*S*)-Configurations Using the Long Wavelength Approximation with the Basis Sets 6-31G*, 6-31G, and DZP from the CADPAC Library[a]**

	6-31G*	6-31G**	DZP	*E* (kJ/mol)
cis-(*R*)-**2**(a)	−37.3	−31.9	−31.7	0.0
cis-(*R*)-**2**(b)	−77.8	−68.5	−48.9	2.6
trans-(*S*)-**3**(a)	−35.0	−28.5	−83.9	0.0
trans-(*S*)-**3**(b)	−0.9	1.4	−8.6	3.1

[a] The molar rotation angles were computed for the geometries obtained from Monte Carlo sampling with an MM2* force field. Also shown is the relative conformational energy (*E*).

dependence and the sensitivity to geometry in these molecules are the subject of ongoing studies.

Table 5 shows the molar rotation angles for 2-methyl azetidine in *cis*-(*R*)- and *trans*-(*S*)-configurations computed for the geometries obtained from Monte Carlo sampling with an MM2* force field. Exhaustive conformational search yields only two possible conformations for this molecule within 50 kJ/mol of the lowest energy structure. The conformations differ by a twist in the four-membered ring. The molar rotation angles computed using the CADPAC program and the MM2* force field optimized geometries predict the right sign but not the right magnitude. The molar rotation angle for the second conformation with the DZP basis set is −8.6, close to the experimental molar rotation of −3.0.

Table 6 shows the molar rotation angles computed using MM3* optimized geometries. The molar rotation angles computed based on MM3* geometries are not accurate either in sign or in magnitude. It can be concluded that the geometries obtained from the MM3* force field in these flexible azetidine ring systems do not lead to a reliable prediction of rotation angle. All of the calculations on the *cis*- and *trans*-2-methyl azetidine indicate the importance of accurate geometry and of basis set selection in obtaining correct molar rotation angles. Despite their deceptively small size, substituted azetidines represent formidable challenges for optical rotation angle computations due to the extreme sensitivity to geometry in these heterocycles.

C. Menthols and Menthones. The optical rotations for menthols and menthones were computed using the long-wavelength approximation. It is interesting to calculate optical rotations for these molecules because of the presence of multiple closely linked chiral centers. Menthol has chiral carbons at positions 2, 4, and 5. Menthone has two chiral centers at positions 2 and 5.

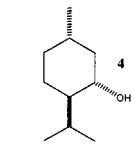

(1*S*,2*R*,5*S*)-(+)-Menthol

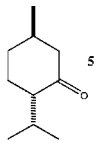

(2*S*,5*R*)-(-)-Menthone

Optical rotations were computed for the geometries obtained from a conformational search using Monte Carlo sampling and the MM2* force field. The Monte Carlo sampling was carried out for both the D- and L-enantiomers of menthol and the D- and L-enantiomers of menthone. The geometry sampling resulted in very few low energy conformers that contributed significantly to the Boltzmann weighted sum that determines the optical rotation angle. This is undoubtedly due to the relatively low degree of conformational flexibility in these molecules.

Table 7 shows the Boltzmann weighted sum of specific rotation angles for D- and L-configurations of menthol and menthone. The last column in Table 7 indicates the corresponding experimental values. The specific rotation angles were computed using a standard 6-31G* basis set in the CADPAC library. The computed specific rotation angle for (1*S*,2*R*,5*S*)-(+)-menthol (**4**) is +33.2 compared to the experimental value of +48.0. The computed specific rotation for (2*S*,5*R*)-(−)-menthone (**5**) is −13.5 compared to an experimental value of −20.0. All of the experimentally measured and the computed specific rotation angles apply for ethanol as a solvent.[61]

TABLE 6: Computed Molar Rotation Angles for Two Conformations (a, b) of 2-Methyl Azetidine in *cis*-(*R*)- and *trans*-(*S*)-Configurations Using the Long-Wavelength Approximation with the Basis Sets 6-31G*, 6-31G, and DZP from the CADPAC Library[a]**

	6-31G*	6-31G**	DZP	*E* (kJ/mol)
cis-(*R*)-**2**(a)	−39.3	−34.9	−57.1	0.0
cis-(*R*)-**2**(b)	−91.3	−82.3	−76.1	3.2
trans-(*S*)-**3**(a)	22.8	25.4	34.3	0.0
trans-(*S*)-**3**(b)	−11.4	−5.7	−53.3	0.4

[a] The geometries for the *cis*- and *trans*-conformations were optimized using the MM3* force field. Also shown is the relative conformational energy (*E*).

TABLE 7: Computed Specific Rotation Angles for Menthols and Menthones Compared to the Experimental Values

	D-configuration	L-configuration	exptl[61]
menthol	33.2	−33.4	(D) +48
menthone	13.5	−13.5	(L) −20

Conclusions

Our examinations of several small organic molecules provide further support for the premise that theory now provides a viable tool to assist in absolute stereochemistry assignment. Moreover, atomic mapping of rotation angle (see Figure 4) pinpoints the structural origins of the rotation angle. Most importantly, we observed, particularly in indoline (**1**) that conformational chirality−asymmetry associated with groups well removed from tetrahedral carbon chiral centers *m* actually controls the *sign* of the rotation angle arising in a specific conformer. This is consistent with earlier studies that emphasized the importance of conformation for rotation angle.[39] In indoline (**1**) a direct correlation between the dihedral angle of the allyl substituent and the sign of the atomic contributions to optical activity was noted. This observation suggests (1) the possibility of manipulating the sign and magnitude of rotation angles by controlling molecular conformation at sites somewhat remote from tetrahedral chiral centers and (2) the prospect of utilizing more subtle information (as yet) buried in ORD data in order to ascertain not only absolute stereochemistry, but also to extract more detailed information about folded molecular structure.

The frequency dependent rotation angles, i.e., the optical rotatory dispersion spectra, are well described in the off-resonance regime by static-field methods. As the frequency approaches electronic resonance, the frequency dependent linear-response methods are more reliable. Our calculations indicate that in indoline (**1**), menthol, and menthone a 6-31G* basis is adequate. However, in azetidine, a 6-31G** basis gives improved results. It is critical to note that the good agreement between theory and experiment cited here is reached only after summing rotation angles over Boltzmann-weighted thermally accessible conformers. Indeed, if only the lowest energy conformer for indoline (**1**) were considered, the sign of the predicted rotation angle would be in error. In the structures with

the greatest conformational freedom examined here, 8−10 structures were needed for the Boltzmann sum to converge. In more rigid structures, such as menthols and menthones, just two structures sufficed. Azetidine serves as an important reminder that in some cases the quality of optical rotation angle calculations can be critically influenced by seemingly minor differences in geometry and basis set selection.

Acknowledgment. We thank the PRF (Grant 33532AC), NSF (Grant CHE-9727657), and NIH (Grant GM 55433) for support of this research, and Prof. Bailey and Mr. Mealy for a preprint of their work. We thank Prof. D. W. Pratt for stimulating discussions.

References and Notes

(1) van't Hoff, J. H. *Arch. Neerl. Sci. Exactes Nat.* **1874**, *9*, 455. van't Hoff, J. H. *Die Lagerung der Atome im Raume*; Vieweg: Braunschweig, Germany, 1894; p 95.
(2) Walden, P. *Z. Phys. Chem.* **1894**, *15*, 196.
(3) Eliel, E. L.; Wilen, S. H.; Mander, L. N. *Stereochemistry of Organic Compounds*; Wiley: New York, 1994.
(4) Nakanishi, K.; Berova, N.; Woody, R. W. *Circular Dichroism Principles and Applications*; VCH Publishers, Inc.: New York, 1994.
(5) Freudenberg, K.; Todd, J.; Seidler, R. *Ann. Chem.* **1933**, *501*, 199.
(6) Brewster, J. H. *Tetrahedron* **1961**, *13*, 106.
(7) Moscowitz, A. *Adv. Chem. Phys.* **1962**, *4*, 67.
(8) Applequest, J. *J. Chem. Phys.* **1973**, *10*, 4251.
(9) Tinoco, I., Jr.; Woody, R. W. *J. Chem. Phys.* **1963**, *40*, 160.
(10) Satyanarayana, B. K.; Stevens, E. S. *J. Org. Chem.* **1987**, *52*, 3170.
(11) Gould, R. R.; Hoffmann, R. *J. Am. Chem. Soc.* **1970**, *92*, 1813.
(12) Pao, Y. H.; Santry, D. P. *J. Am. Chem. Soc.* **1966**, *88*, 4157.
(13) Kuhn, W. In *Stereochemie*; Freudenberg, K., Ed.; Deuticke: Leipzig, 1933; Vol. 8, p 394.
(14) Born, M. *Proc. R. Soc. London, Ser. A* **1935**, *150*, 84.
(15) Kirkwood, J. G. *J. Chem. Phys.* **1937**, *5*, 479.
(16) Nolte, H. J.; Buss, V. *Tetrahedron* **1974**, *31*, 719.
(17) Maestro, M.; Moccia, R.; Taddei, G. *Theor. Chim. Acta* **1967**, *8*, 80.
(18) Kondru, R. K.; Lim, S.; Wipf, P.; Beratan, D. N. *Chirality* **1997**, *9*, 469.
(19) Rauk, A.; Barriel, J. M. *Chem. Phys.* **1977**, *25*, 409.
(20) Bak, K. L.; Hansen, Aa. E.; Ruud, K.; Helgaker, T.; Olsen, J.; Jørgensen, P. *Theor. Chim. Acta* **1995**, *90*, 441.
(21) Hansen, A. E.; Bouman, T. D. *J. Am. Chem. Soc.* **1985**, *107*, 4828.
(22) Snatzke, G. In *Chirality: from Weak Bosons to the Alpha-Helix*; Janoschek, Ed.; Springer Verlag: Berlin, Germany, 1991; pp 59−85.
(23) Costante, J.; Hecht, L.; Polavarapu, P. L.; Collet, A.; Barron, L. D. *Angew. Chem., Int. Ed. Engl.* **1997**, *36*, 885.
(24) Polavarapu, P. L. *Mol. Phys.* **1997**, *91*, 551.
(25) Polavarapu, P. L. *Tetrahedron: Asymmetry* **1997**, *8*, 3397.
(26) Polavarapu, P. L.; Chakraborty, D. K. *J. Am. Chem. Soc.* **1998**, *120*, 6160.
(27) Kondru, R. K.; Wipf, P.; Beratan, D. N. *J. Am. Chem. Soc.* **1998**, *120*, 2204.
(28) Polavarapu, P. L.; Zhao, C. *J. Am. Chem. Soc.* **1999**, *121*, 246.
(29) Rosenfeld, L. *Z. Physik* **1928**, *52*, 161.
(30) Lakhtakia, A., Ed. *Selected Papers on Natural Optical Activity*; SPIE Milestone Series MS 15; SPIE Press: Bellingham, WA, 1990.
(31) Eyring, H.; Walter, J.; Kimball, G. E. *Quantum Chemistry*; Wiley, New York, 1944.
(32) Rodger, A.; Nordén, B. *Circular Dichroism and Linear Dichroism*; SPIE Milestone Series MS 15; Oxford University Press: Oxford, 1997.
(33) Arndt, E. R.; Stevens, E. S. *Biopolymer* **1994**, *34*, 1527. Arndt, E. R.; Stevens, E. S. *Biopolymer* **1996**, *38*, 567.
(34) Johnson, W. C.; Tinoco, I. *J. Am. Chem. Soc.* **1972**, *94*, 4389.
(35) Shellman, J. A. *J. Chem. Phys.* **1966**, *44*, 55.
(36) Nafie, L. A. *Annu. Rev. Phys. Chem.* **1997**, *48*, 357.
(37) Bormett, R. W.; Asher, S. A.; Larkin, P. J.; Williams, G. G.; Ragunathan, N.; Freedman, T. B.; Nafie, L. A.; Balasubramanian, S.; Boxer, S. G.; Yu, N. T.; Gersonde, K.; Noble, R. W.; Springer, B. A.; Sligar, S. G. *J. Am. Chem. Soc.* **1992**, *114*, 6864.
(38) Brewster, J. H. *J. Am. Chem. Soc.* **1959**, *81*, 5475.
(39) Kauzmann, W.; Eyring, H. *J. Chem. Phys.* **1941**, *9*, 41.
(40) Schafer, S. E.; Stevens, E. S. *Biopolym.* **1995**, *36*, 103.
(41) Polavarapu, P. L.; Zhao, C. *J. Chem. Phys.* **1999**, *121*, 246.
(42) Kondru, R. K.; Wipf, P.; Beratan, D. N. *Science* **1998**, *282*, 2247.
(43) Amos, R. D.; Rice, J. E. *The Cambridge Analytic Derivative Package*, Release 4.0; Cambridge University: Cambridge, 1987.
(44) Helgaker, T.; Jensen, H. J. A.; Olsen, J.; Ruud, K.; Anderson, A. T.; Bak, K. L.; Bakken, V.; Christiansen, O.; Dahle, P.; Dalskov, E. K.; Enevoldsen, T.; Fernandez, B.; Heiberg, H.; Hettema, H.; Jonsson, D.; Kirpekar, S.; Kobayashi, R.; Koch, H.; Mikkelsen, K. V.; Norman, P.; Packer, P.; Saue, T.; Taylor, P. R.; Vahtras, O.; *Dalton, an* ab initio *electronic structure program*, Release 1.0; 1997.
(45) Amos, R. D. *Chem. Phys. Letters* **1982**, *87*, 23.
(46) Linderberg, J.; Öhrn, Y. In *Propagators in Quantum Chemistry*; Academic Press: New York, 1973.
(47) Olsen, J.; Jørgensen, P. *J. Chem. Phys.* **1985**, *82*, 3235.
(48) Jørgensen, P.; Jensen, H. J. A.; Olsen, J. *J. Chem. Phys.* **1988**, *89*, 3654.
(49) Helgaker, T.; Ruud, K.; Bak, K. L.; Jørgensen, P.; Olsen, J. *Faraday Discuss.* **1994**, *99*, 165.
(50) Amos, R. D. *Chem. Phys. Lett.* **1982**, *87*, 23.
(51) London, F. *J. Phys. Radium.* **1937**, *8*, 397.
(52) Bak, K. L.; Jørgensen, P.; Helgaker, T.; Ruud, K. *Faraday Discuss.* **1994**, *99*, 121.
(53) Amos, R. D. *Chem. Phys. Letters* **1986**, *124*, 376.
(54) Mulliken, R. S. *J. Chem. Phys.* **1955**, *23*, 1833. Mulliken, R S. *J. Chem. Phys.* **1962**, *36*, 3428. Pople, J. A.; Beveridge, D. L. *Approximate Molecular Orbital Theory*; McGraw-Hill: New York, 1970.
(55) Mohamadi, F.; Richards, N. G. J.; Guida, W. C.; Liskamp; R. Caufield, C.; Chang, G.; Hendrickson, T.; Still, W. C. *J. Comput. Chem.* **1990**, *11*, 440.
(56) Pettersson, I., Liljefors, T. In *Reviews in Computational Chemistry*; Lipkowitz, K. B., Boyd, D. B., Eds.; VCH: New York, 1996; Vol. 9, pp 167.
(57) Still, W. C.; Tempczyk, A.; Hawley, R. C.; Hendrickson, T. *J. Am. Chem. Soc.* **1990**, *112*, 6127.
(58) Bailey, W. F. The University of Connecticut. Private communication. Bailey, W. F.; Mealy, M. J.; Submitted for publication.
(59) Kumata, Y.; Furukawa, J.; Fueno, T. *Bull. Chem. Soc. Jpn.* **1970**, *43*, 3920.
(60) Kostyanovsky, R. G.; Markov, V. I.; Gella, I. M. *Tetrahedron Lett.* **1972**, 1301.
(61) Experimental specific rotation angles for D-menthol and L-menthone were taken from the 1997 Aldrich catalogue.